

CH₄ and CO₂ Adsorption Study in ZIF-8 and Al-BDC MOFs

Autié Castro G.¹, de Oliveira Jardim E.², Reguera E.^{1,3}, Vilarrasa-García E.², Rodríguez-Castellón E.^{4*}, Cavalcante Jr. C.L.²

1. Institute of Science and Technology of Materials (IMRE), University of Havana, 10400 Havana, Cuba.

2. Universidade Federal do Ceará, Department of Chemical Engineering, GPSA-Group of Research in Separations by Adsorption, Campus do Pici, 60455760 Fortaleza, Ceará, Brazil.

3. Center for Applied Science and Advanced Technologies of IPN, 11500, Mexico, DF.

4. Department of Inorganic Chemistry, Crystallography and Mineralogy, Faculty of Sciences, University of Malaga, Campus de Teatinos, 29071, Malaga, Spain.

Received: June 22, 2017 / Accepted: July 21, 2017 / Published: September 25, 2017

Abstract: CH₄ and CO₂ adsorption capacity at 25, 50 and 75°C was evaluated in two metal-organic frameworks: Al-BDC and ZIF-8, the later with zeolite topology. Adsorption experiments were carried out under static conditions using a gravimetric suspension balance until 40 bar of pressure. Adsorption isotherms of type I were obtained for both materials showing high adsorption capacity values. ZIF-8 exhibited the higher uptake value for both CH₄ and CO₂ (4.9 and 8.5 mmol g⁻¹, respectively). The Toth equilibrium model was used to fit experimental isotherms in order to obtain q_m (maximum adsorption capacity) and t (related to energetical heterogeneity of the surface). Isothermic heats of adsorption were also calculated by Clausius-Clapeyron equation.

Keywords: Adsorption, ZIFs, MOFs, adsorption heats, adsorption isotherm

1. Introduction

A new family of materials named metal organic framework (MOFs) has been developed principally in the last two decades. These novel crystalline materials attract the scientific interest because of it is possible to design rationally new structures as well as to monitor the empty spaces (pores and cavities) at nanometrical

Corresponding author: Prof. Enrique Rodríguez-Castellón. Departamento de Química Inorgánica, Facultad de Ciencias, Universidad de Málaga, 29071 Málaga, Spain. Tel.: +34 952131873. E-mail: castellon@uma.es.

scale. The control of the empty spaces enables the manipulation capacity of the molecule chemistry trapped inside which represents a powerful tool for several important applications.

MOFs are composed of two blocks: (i) the connectors (ligands) and (ii) nodes (metallic ions with charge ²⁺ or ³⁺) which constitute open metal sites located at the cavities surface. The strength of the bond between the metal oxide cluster and the linker has been suggested to be important in determining the stability [1]. They are attractive for adsorption and separation applications [2-5] and gases storage [6, 7] due to their thermal and chemical stability, versatility and numerous structural design possibilities.

The framework structure of MIL-53-Al (also known as Al-BDC) is composed of infinite AlO₄(OH)₂ octahedra connected by a 1,4-benzenedicarboxylate ligand. Its chemical formula is M(OH)(O₂C-C₆H₄-CO₂), in which M stands for either Al³⁺ [8]. This MOF is important in the field of gas adsorption [9, 10] and separation of organic compounds [11].

More recently a MOFs sub-family known as ZIFs (zeolitic imidazolate frameworks) has fascinated the scientific community. These materials own a zeolitic type structure given by their structure similarity with these inorganic compounds and possess even higher thermal stability. Their framework arises by the metallic node connected by imidazole derivatives with a tetrahedral environment [12].

The zinc 2-methylimidazolate [Zn(C₄H₅N₂)₂ or Zn(MeIm)₂], zeolitic imidazolate framework ZIF-8 [13, 14] is commercially available, highly stable MOF that is receiving great interest for a diverse variety of applications. ZIF-8 is constructed from corner-sharing Zn(MeIm)₄ tetrahedral units in which the MeIm-ligands bridge the Zn²⁺ ions to form a three-dimensional framework with the sodalite framework topology and a pore size of 3.4 Å. Separation of linear and branched alkanes, ethane/ethylene, hydrogen storage and carbon dioxide capture have been evaluated using ZIF-8 material [12, 15-17].

From an environmental and energy perspective, purification and recovery of carbon dioxide from flue gas and natural gas are of great interest. CO₂ is the main component of the greenhouse gases, and its accumulation in the environment is leading to global warming issues. Thus, the selective adsorption of CH₄ in the presence of other gas species, such as CO₂, is a property of fundamental interest. Methane adsorption and selectivity in ZIFs have been studied both experimentally [18] and computationally [19] for pure gases and gas mixtures relevant in the context of natural gas separations. Experimental studies in ZIFs have involved measurements of adsorption isotherms [18], breakthrough curves [20], and membrane selectivity [21]. The understanding derived from these studies has been complemented by relevant investigations in other related metal-organic framework (MOF) systems, [22, 23] featuring data on the time-resolved uptake of methane and carbon dioxide [24] as well as neutron scattering to characterize CH₄ and CO₂ binding sites and occupations [25, 26]. The studies of ZIFs have shown that these frameworks can exhibit adsorption

selectivities and uptakes that exceed the performance of commercial adsorbents used for natural gas separation and that performance depends on several factors, including the choice of linker, functionalization, pore size, and metal ion.

In this work, a gravimetric adsorption study of CH₄ and CO₂ using ZIF-8 and Al-BDC MOFs is exposed. Adsorption and desorption isotherms at 25, 50 and 75°C up to 40 bar of pressure were obtained. From the recorded isotherms the adsorption heats (Q_d) were estimated using the Clausius Clapeyron's equation. The Toth model was used to fit the experimental isotherms in order to obtain q_m (maximum adsorption capacity) and t (parameter related to energetical heterogeneity of the surface).

2. Materials and Methods

2.1 Materials

ZIF-8 and Al-BDC were supplied by Sigma-Aldrich (commercialized as Basolite Z1200 and Basolite A100; Cat. Nr.59061-53-9 and Cat. Nr. 185361, respectively). Table 1 summarizes some textural properties of both materials: specific surface area and micropore volume [27, 28].

Table 1. Textural properties.

Material	Specific Surface area and micropore volume		Reference
	Surface area (m ² ·g ⁻¹)	Micropore volume (cm ³ ·g ⁻¹)	
<i>Al-BDC</i>	1100	0.350	[27]
<i>ZIF-8</i>	1813	0.663	[28]

2.2 Methods

Scanning electron microscope (SEM) observation was conducted on a Philips CM 200 Supertwin-DX4, from samples dispersed in ethanol. A drop of the suspension was put on a carbon coated Cugrid (300 mesh).

The conditions of sample regeneration and thermal stability were evaluated from thermogravimetric curves (TG) recorded using a thermal analyzer METTLER TOLEDO, model TGA/DSC 1 with software STARE version 10.00 from METTLER TOLEDO STAR[®] system. The experiments were carried out in N₂ at flow of 50 ml·min⁻¹ with a rate of 10°C·min⁻¹.

CH₄ and CO₂ adsorption experiments were carried out using a magnetic suspension balance Rubotherm (Bochum, Germany). Adsorption measurements were performed at 25, 50 and 75°C until 40 bar. Prior to

each measurement samples were outgassed 200°C (heating rate of 2°C.min⁻¹) under vacuum (10⁻³ bar). Experimental data were obtained gravimetrically so it was necessary to take into account the effects of buoyancy during the experiments. For a given pressure P of surrounding gas, the adsorbed phase concentration in excess could be obtained according to (Eq. 1):

$$m_{ex}(P,T) = \Delta m (P,T) + (V_b + V_s) \cdot \rho(P,T) \quad (1)$$

where:

m_{ex} : excess mass amount adsorbed (g.g⁻¹ of sample)

Δm : mass difference recorded by the equipment (g.g⁻¹ of sample)

V_b : specific volume of the balance suspended components (cm³.g⁻¹ of sample)

V_s : specific volume of the solid sample (cm³.g⁻¹ of sample)

ρ : gas density (g.cm⁻³)

P : pressure (bar)

T : temperature (K)

The absolute mass was estimated using the standard procedure reported by Myers et al. (Eq. 2) [29].

$$n_a = n_e + \rho v_p \quad (2)$$

where $v_p = V_{mp}/m_s$ is the specific micropore volume (cm³.g⁻¹) of the solid.

Isothermic heats of adsorption were obtained using the Clausius Clapeyron's equation (Eq. 3):

$$d(\ln P)/dT = \Delta H/RT^2 \quad (3)$$

Experimental isotherms were fitted to the Toth model as (Eq. 4) [30].

$$q = q_m \frac{bP}{(1+(bP)^t)^{1/t}} \quad (4)$$

where:

q_m : maximum adsorption capacity

b : parameter related to the affinity of the pair adsorbate-adsorbent

t : parameter related to energetical heterogeneity of the surface

Binary isotherms were predicted by the Toth extended model (Eq 5)

$$q_i = \frac{q_{max,i} b_i P_i}{(1 + \sum_{i=1}^J (b_i P_i)^{t_i})^{1/t_i}} \quad (5)$$

The efficiency of carbon dioxide separation for these MOFs was estimated by the selectivity of CO₂ over CH₄ considering a scenario of 70% CH₄ and 30 % CO₂ (v/v). Selectivity was calculated from the ratios of mole fractions in the gas phase and in the adsorbed phase at equilibrium, as shown in (Eq. 6):

$$S_{i/j} = \frac{q_{i \text{ mixt}}}{q_{j \text{ mixt}}} * \frac{P_j}{P_i} \quad (6)$$

3. Results and Discussion

SEM images of the ZIF-8 and Al-BDC solids morphology are showed in Figure 1 (a) and (b), respectively. SEM study revealed the presence of clusters of spherical and uniform particles of size between 180-240 nm in the case of ZIF-8 sample, (Figure 1a). However, the Al-BDC material showed an irregular morphology of different size particles, (Figure 1b).

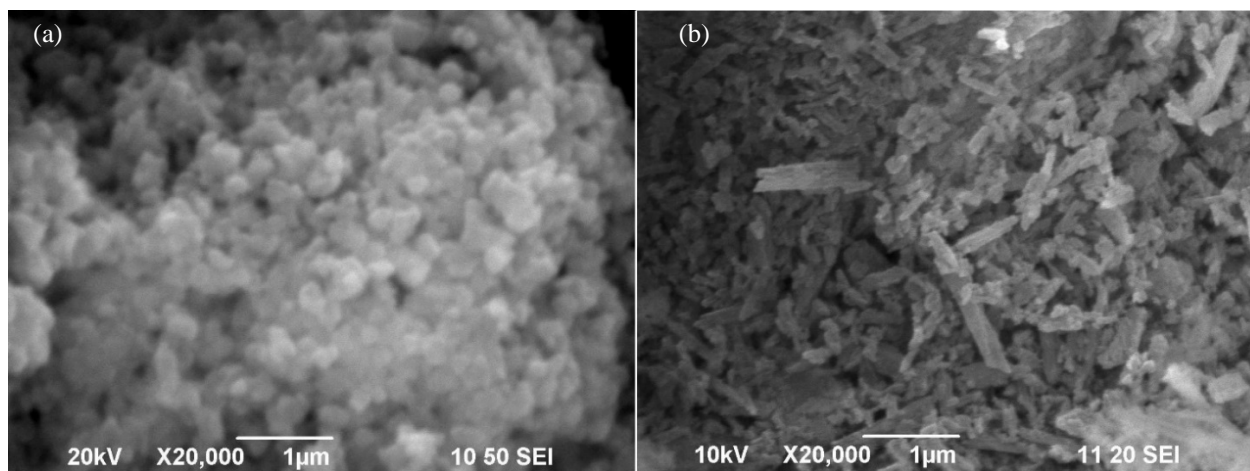


Fig. 1:SEM micrographs (a): ZIF-8 and (b): Al-BDC.

Thermal stability of ZIF-8 and Al-BDC was evaluated by thermogravimetric analysis (TGA). The weight loss percent of both materials as a function of the temperature is shown in Figure 2. For temperatures between 40-230°C; 230-420°C and 420-470°C continuous weight losses of 6 %, 6 % and 54 %, respectively, were observed for the ZIF-8 sample, which is attributed to water and residual solvent used in the synthesis process. On the other hand, the Al-BDC sample showed just two individual weight losses of 11 % and 49 %, within temperatures between 30-536°C and 536-677°C, respectively, attributed to the removal of water and the solvents used in the synthesis.

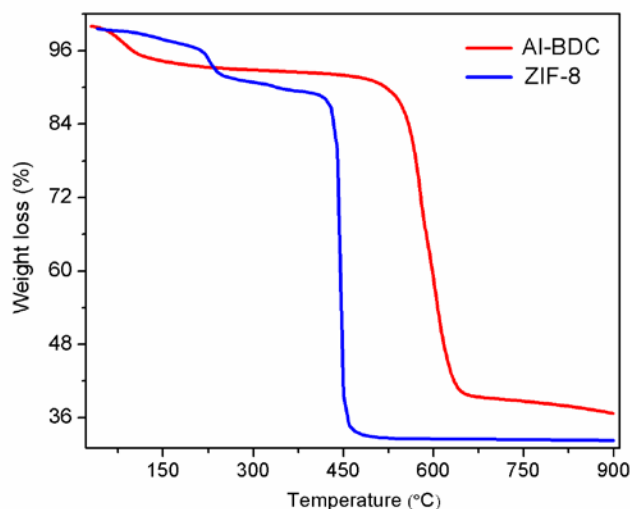


Fig. 2: Thermogravimetric curves of ZIF-8 and Al-BDC.

CO₂ and CH₄ single component adsorption and desorption isotherms at 25, 50 and 75°C are shown in Figure 3 in the range of pressures between 0-40 bars. As expected, both samples exhibited preferential adsorption for CO₂ in relation to CH₄ over the whole pressure range for all measured temperatures. ZIF-8 sample exhibited the highest adsorption capacity of CO₂ under the studied conditions (8.5 mmol.g⁻¹ for CO₂ and 4.7 mmol.g⁻¹ for CH₄ at 25°C and 40 bar). Additionally, it was appreciated that the ZIF-8 presented a higher CO₂ adsorption capacity than that observed for the Al-BDC sample (5 mmol.g⁻¹ of CO₂ under the same conditions). This higher CO₂ capture capacity may be attributed to the combination of high specific surface area and micropore volume. Similar behavior has been reported in ZIF-69 and ZIF-76 at 30°C [31]. All isotherms do not present hysteresis loop indicating the reversibility of process.

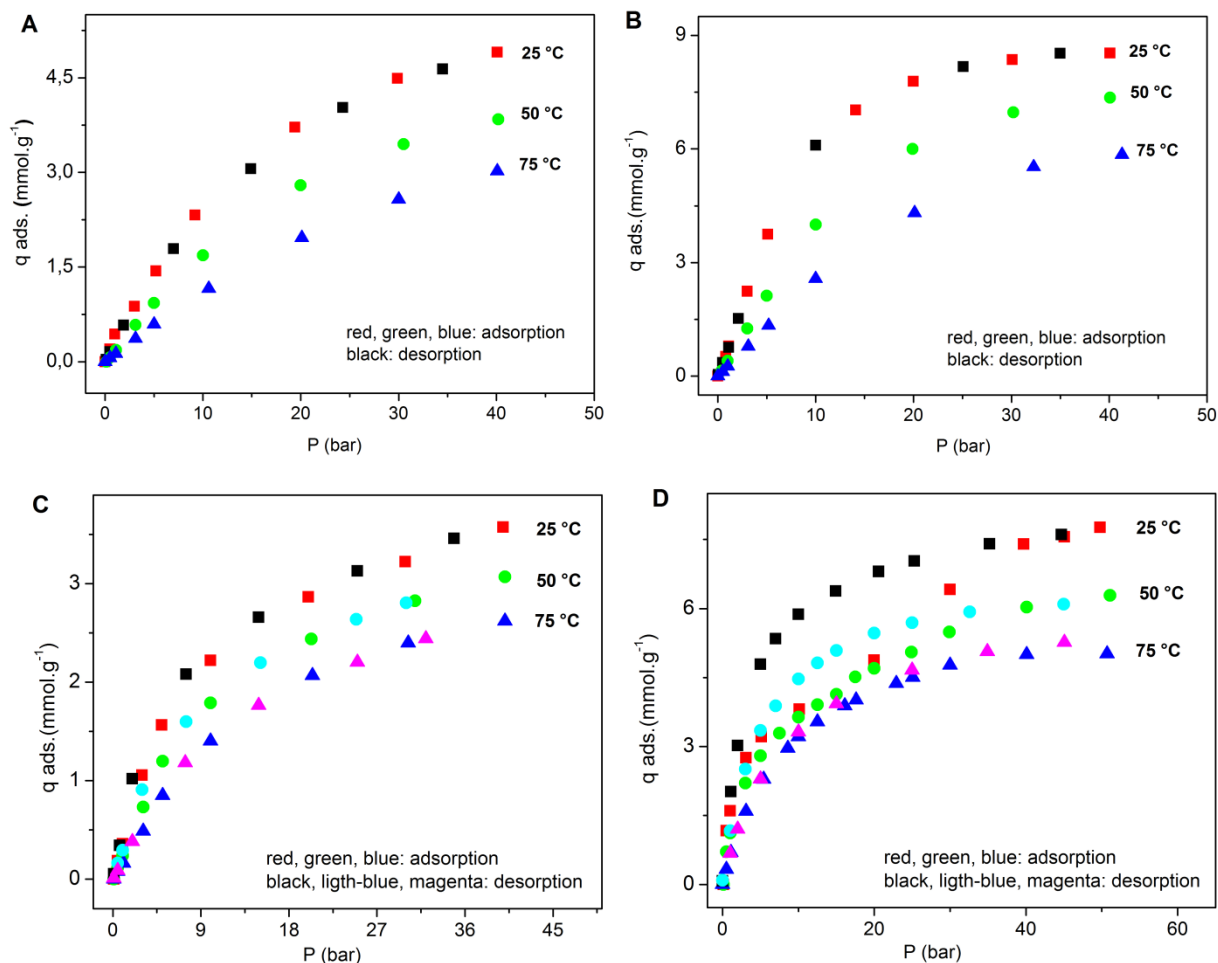


Fig. 3: Single component adsorption isotherms of A: CH₄, B: CO₂ in ZIF-8 and C: CH₄, D: CO₂ in Al-BDC at 25, 50 and 75°C until 40 bar of pressure.

The Both parameters and the isosteric heats of adsorption for both samples are summarized in Table 2 and Figure 4. The parameter b (Eq. 4) indicates how strongly the adsorbate molecule is attracted onto adsorbent surface [30]. As expected, higher b values were obtained for CO₂ in comparison with CH₄. This behavior could be ascribed to the presence of a quadrupolar moment in the CO₂ molecule which could interact with the electric field gradient inside the pores and cavities. The CH₄ molecule presents octupolar moment which is smaller in magnitude than the quadrupolar moment of the CO₂ molecule ($Q_{zz,CO_2} = 5.9 \times 10^{-26}$ esu cm², $\Omega_{CH_4} = 6 \times 10^{-34}$ esu cm³) [32]. For each sample, it can also be observed that higher values for q_{max} are obtained for CO₂. The isosteric heats of adsorption for CO₂ were higher than those for CH₄ in the two studied samples; and they were higher in the ZIF-8 material. These results could be related to the higher specific surface area as well as the higher micropore volume in this material. A lower heat of adsorption usually means an easier

regeneration and from the observed behavior, one can conclude that these MOFs have not only high capacity and apparent selectivity for CO₂ but also potentially a good regenerability.

Table 2. Parameters of Toth isotherm model, calculated selectivity (CO₂/CH₄) and isosteric heats of adsorption for ZIF-8 and Al-BDC MOFs.

Sample (V_{mp} ($\text{cm}^3 \cdot \text{g}^{-1}$))	Toth parameters					Selectivity (mol CO ₂ /mol CH ₄) ^a	Adsorption heats
ZIF-8 (0.58)	$T(^{\circ}\text{C})$	$q_m(\text{mmol} \cdot \text{g}^{-1})$	$b(\text{bar}^{-1})$	t	r^2		$Q_d(\text{kJ} \cdot \text{mol}^{-1})$
CO ₂	25	14.31	0.065	0.98	0.96543	2.21	
	50	14.02	0.040	0.98	0.97581	2.11	-19.5
	75	13.91	0.024	0.98	0.99012	1.71	
CH ₄	25	9.98	0.043	0.93	0.98991		
	50	9.02	0.030	0.91	0.98753		-17.0
	75	8.01	0.025	0.90	0.98021		
Al-BDC(0.325)	$T(^{\circ}\text{C})$	$q_m(\text{mmol} \cdot \text{g}^{-1})$	$b(\text{bar}^{-1})$	t	r^2		$Q_d(\text{kJ} \cdot \text{mol}^{-1})$
CO ₂	25	15.32	0.101	0.57	0.94565	2.33	
	50	13.21	0.094	0.57	0.95871	2.92	-15.0
	75	11.41	0.093	0.57	0.97244	3.68	
CH ₄	25	5.17	0.084	1.00	0.99454		
	50	5.04	0.058	1.00	0.99956		-13.5
	75	5.01	0.041	1.00	0.99745		

^a: average values calculated in the pressure range from 0.1 to 30 bar

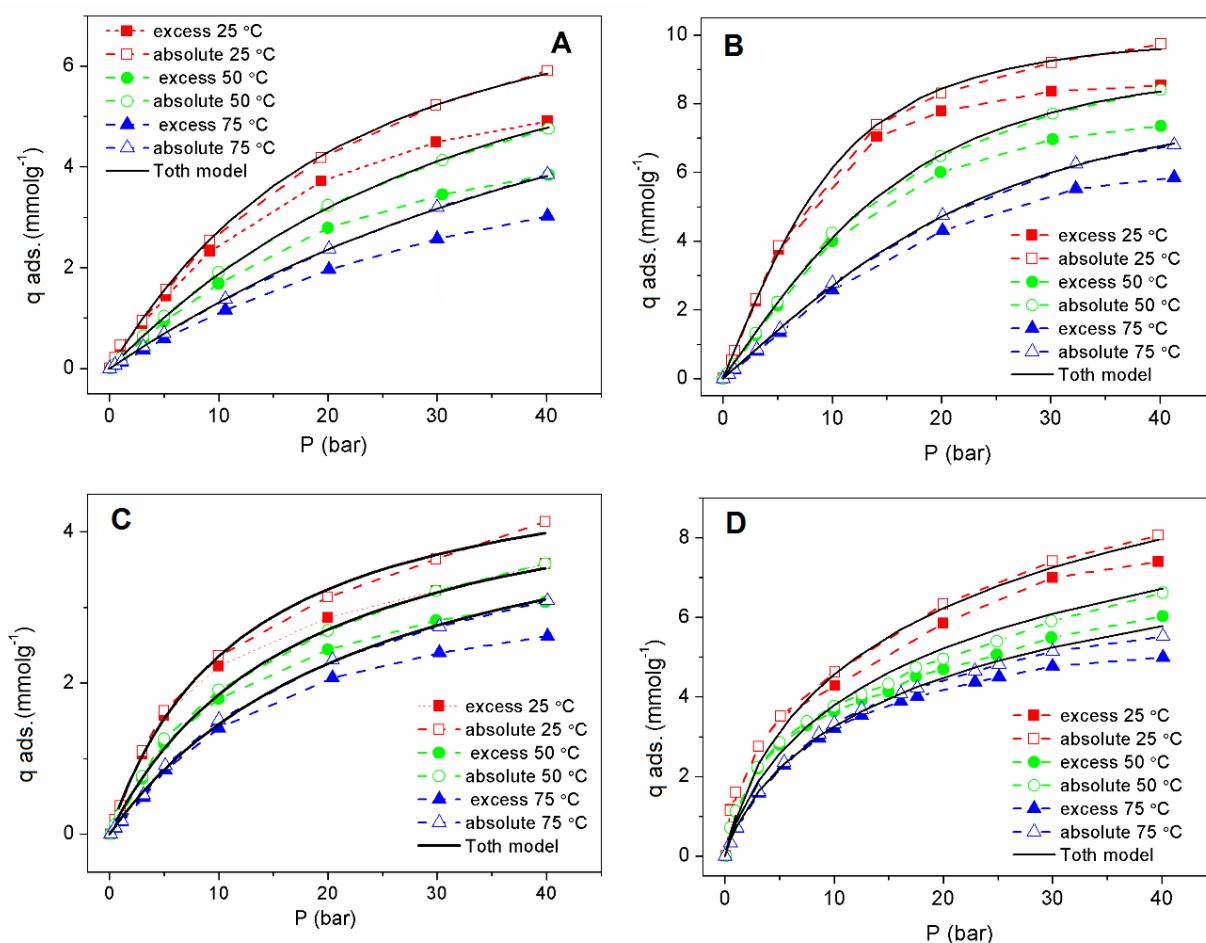


Fig. 4: Representation of Toth model for the obtained isotherms of CH₄ and CO₂ adsorbates in ZIF-8 and Al-BDC MOFs. A: CH₄ in ZIF-8, B: CO₂ in ZIF-8, C: CH₄ in Al-BDC and D: CO₂ in Al-BDC.

From the fit of the Toth model, several mixture isotherms were simulated at different temperatures (Figure 5). From this, binary gas equilibrium adsorption isotherms were obtained at 25, 50 and 75 °C for an ideal gas natural composition (30% CO₂ and 70% CH₄). The aim of this study is to check if these materials have the same trend when the mixture evolves towards higher temperatures. Al-BDC and ZIF-8 samples showed, as expected, a decrease in the gravimetric uptake as the temperature increases, especially in the case of ZIF-8. In terms of selectivity, the Toth extended model predicts for ZIF-8 a decreasing selectivity as temperature increases while for the Al-BDC material this behavior is not observed, the selectivity increases as the temperature increases. The highest CO₂ affinity of this MOF balances the loss of CO₂ capacity when the temperature increases, remaining a high CO₂/CH₄ selectivity and even improves it.

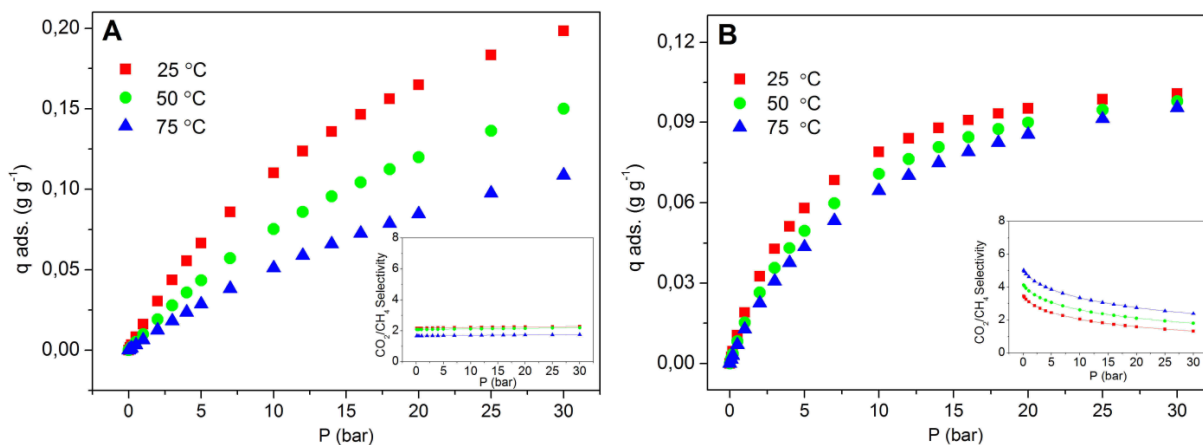


Fig 5: CO₂/CH₄ (30/70 v/v) binary isotherms predicted by Toth Extended model for A: ZIF-8 and B: Al-BDC.

CO₂/CH₄ selectivity values are also plotted.

4. Conclusion

CH₄ and CO₂ adsorption at 25, 50 and 75 °C up to 40 bar of pressure were carried out using Al-BDC and ZIF-8 MOFs as adsorbents. Both materials showed optimal levels of adsorption; therefore the two evaluated adsorbents seem to be attractive for CH₄ and CO₂ adsorption. However ZIF-8 exhibited higher CO₂ capture capacity under the studied conditions. This fact may be attributed to the combination of high specific surface area and micropore volume. Experimental isotherms were fitted to the Toth model from which higher b values were obtained for CO₂ in comparison with CH₄. Since the b parameter indicates how strongly the adsorbate molecule is attracted onto the adsorbent surface this could be related to the presence of a quadrupolar moment in the CO₂ molecule which would interact more strongly with the electric field gradient inside the pores and cavities.

Acknowledgments

Thanks to UNESCO/Keizo Obuchi Research Fellowships Programme (UNESCO/Japan Young Researcher's Fellowship Program), Cycle 2012, Programa de Becas para la realización de la tesis doctoral en la Universidad de Málaga convocatoria curso 2011-2012 (AUIP-UMA), European project 295156, FP7-PEOPLE-2011-IRSES and MINECO, Spain, Project CTQ2015-68951-C3-3-R and FEDER funds. Dr. Giselle Autié Castro thanks to CNPq-TWAS Postdoctoral Fellowship 2014 and its financial support.

References

- [1] J. J. Low et al. Virtual high throughput screening confirmed experimentally: porous coordination polymer hydration. *J. Am. Chem. Soc.* 131(43) (2009) 15834-15842.
- [2] Z. Zhang et al. MOFs for CO₂ capture and separation from flue gas mixtures: the effect of multifunctional sites on their adsorption capacity and selectivity. *Chem. Commun.* 49 (2013) 653-661.
- [3] L. Pan et al. Zn(tbip) (H₂tbp=5-*tert*-Butyl Isophthalic Acid): A Highly Stable Guest-Free Microporous Metal Organic Framework with Unique Gas Separation Capability. *J. Am. Chem. Soc.* 128 (2006) 4180-4181.
- [4] J. Y. Lee et al. Microporous Metal-Organic Frameworks with High Gas Sorption and Separation Capacity. *Adv. Funct. Mater.* 17 (2007) 1255-1262.
- [5] G. Autie et al. Cu-BTC and Fe-BTC metal-organic frameworks: Role of the materials structural features on their performance for volatile hydrocarbons separation. *Colloids and Surfaces A: Physicochem. Eng. Aspects* 481 (2015) 351-357.
- [6] J. Getzschmann et al. Methane storage mechanism in the metal-organic framework Cu₃(btc)₂: An in situ neutron diffraction study. *Microporous and Mesoporous Materials* 136 (2010) 50-58.
- [7] D. Britt et al. Highly efficient separation of carbon dioxide by a metal-organic framework replete with open metal sites. *Proc. Nat. Acad. Sci. U.S.A.* 106 (49) (2009) 20637-20640.
- [8] T. Loiseau et al. A rationale for the large breathing of the porous aluminum terephthalate (MIL-53) upon hydration. *Chemistry*, 10 (6) (2004) 1373-1382.
- [9] S. Bourrelly et al. Different adsorption behaviors of methane and carbon dioxide in the isotopic nanoporous metal terephthalates MIL-53 and MIL-47. *J. Am. Chem. Soc.* 127 (39)(2005) 13519-13521.
- [10] G. Férey et al. Hydrogen adsorption in the nanoporous metal-benzenedicarboxylate M(OH)(O₂C-C₆H₄-CO₂) (M = Al³⁺, Cr³⁺), MIL-53. *Chem. Commun.* 24 (2003) 2976-2977.
- [11] L. Alaerts et al. Selective adsorption and separation of *ortho*-substituted alkylaromatics with the microporous aluminum terephthalate MIL-53. *J. Am. Chem. Soc.* 130 (2008) 14170-14178.
- [12] R. Banerjee et al. High-Throughput Synthesis of Zeolitic Imidazolate Frameworks and Application to CO₂ Capture. *Science* 319 (2008) 939-943.
- [13] H. Xiao-Chun et al. Ligand-Directed Strategy for Zeolite-Type Metal-Organic Frameworks: Zinc(II) Imidazolates with Unusual Zeolitic Topologies. *Angew. Chem. Int. Ed.* 45 (2006) 1557-1559.
- [14] K. S. Park et al. Exceptional chemical and thermal stability of zeolitic imidazolate frameworks. *Proc. Nat. Acad. Sci. U.S.A.* 103 (2006) 10186-10191.

- [15] N. Chang et al. Zeolitic Imidazolate Framework-8 Nanocrystal Coated Capillary for Molecular Sieving of Branched Alkanes from Linear Alkanes along with High-Resolution Chromatographic Separation of Linear Alkanes. *J. Am. Chem. Soc.* 132 (39) (2010) 13645-13647.
- [16] H. Bux et al. Ethene/ethane separation by the MOF membrane ZIF-8: Molecular correlation of permeation, adsorption, diffusion. *Journal of Membrane Science* 369 (2011) 284-289.
- [17] H. Wu et al. Hydrogen Storage in a Prototypical Zeolitic Imidazolate Framework-8. *J. Am. Chem. Soc. Commun.* 129 (2007) 5314-5315.
- [18] S. R. Venna et al. Highly Permeable Zeolite Imidazolate Framework-8 Membranes for CO₂/CH₄ Separation. *J. Am. Chem. Soc.* 132 (2010) 76-78.
- [19] W. Thornton et al. Feasibility of Zeolitic Imidazolate Framework Membranes for Clean Energy Applications. *Energy Environ. Sci.* 5 (2012) 7637-7646.
- [20] H. Hayashi et al. Zeolite A Imidazolate Frameworks. *Nat. Mater.* 6 (2007) 501-506.
- [21] T. H. Bae et al. A High-Performance Gas-Separation Membrane Containing Submicrometer-Sized Metal-Organic Framework Crystals. *Angew. Chem. Int. Ed.* 49 (2010) 9863-9866.
- [22] Z. Bao et al. Adsorption of CO₂ and CH₄ on a Magnesium- Based Metal Organic Framework. *J. Colloid Interface Sci.* 353 (2011) 549-556.
- [23] E. J. García et al. Role of Structure and Chemistry in Controlling Separations of CO₂/CH₄ and CO₂/CH₄/CO Mixtures over Honeycomb MOFs with Coordinatively Unsaturated Metal Sites. *J. Phys. Chem. C* 116 (2012) 26636-26648.
- [24] Z. Bao et al. Kinetic Separation of Carbon Dioxide and Methane on a Copper Metal-Organic Framework. *J. Colloid Interface Sci.* 357 (2011) 504-509.
- [25] H. Wu et al. High-Capacity Methane Storage in Metal-Organic Frameworks M2 (Dhtp): The Important Role of Open Metal Sites. *J. Am. Chem. Soc.* 131 (2009) 4995-5000.
- [26] H. Wu et al. Adsorption Sites and Binding Nature of CO₂ in Prototypical Metal Organic Frameworks: A Combined Neutron Diffraction and First Principles Study. *J. Phys. Chem. Lett.* 1 (2010) 1946-1951.
- [27] T. Sun et al. Expanding Pore Size of Al-BDC Metal-Organic Frameworks as a Way to Achieve High Adsorption Selectivity for CO₂/CH₄ Separation. *J. Phys. Chem. C* 118 (2014) 15630-15639.
- [28] K. Sung Park et al. From the Cover: Exceptional chemical and thermal stability of zeolitic imidazolate frameworks. *PNAS* 103 (2006) 10186-10191.
- [29] A. L. Myers and P. A. Monson. Physical Adsorption of Gases: The Case for Absolute Adsorption as the Basis for Thermodynamic Analysis. *Adsorption* 20 (4) (2014) 591-622.
- [30] J. Toth. State Equations of the Solid-gas Interface Layers. *Acta Chim. Acad. Sci. Hung.* 69 (1971) 311-328.

- [31] J. Pérez-Pellitero et al. Adsorption of CO₂, CH₄, and N₂ on Zeolitic Imidazolate Frameworks: Experiments and Simulations. *Chem. Eur. J.* 16 (2010) 1560-1571.
- [32] G. Birnbaum et al. Collision-Induced Microwave Absorption in Compressed Gases. II. Molecular Electric Quadrupole Moments, *J. Chem. Phys.* 8 (36) (1962) 2032-2036.